Chemosphere 206 (2018) 447–456

Contents lists available at ScienceDirect

Chemosphere

journal homepage: www.elsevier.com/locate/chemosphere

Dual element (C–Cl) isotope approach to distinguish abiotic reactions of chlorinated methanes by Fe(0) and by Fe(II) on iron minerals at neutral and alkaline pH

Diana Rodríguez-Fernández [a, *], Benjamin Heckel [b], Clara Torrentó [c], Armin Meyer [b], Martin Elsner [b], Daniel Hunkeler [c], Albert Soler [a], Mònica Rosell [a], Cristina Domènech [a]

[a] Grup MAiMA, Mineralogia Aplicada, Geoquímica i Geomicrobiologia, Departament de Mineralogia, Petrologia i Geologia Aplicada, Facultat de Ciències de la Terra, Martí Franquès s/n, Universitat de Barcelona (UB), 08028 Barcelona, Spain
[b] Institute of Groundwater Ecology, Helmholtz Zentrum München, 85764 Neuherberg, Germany
[c] Centre d'hydrogéologie et de géothermie, Université de Neuchâtel, Neuchâtel 2000, Switzerland

HIGHLIGHTS

- Carbon tetrachloride (CT) and chloroform (CF) C and Cl isotope fractionation study.
- CT and CF abiotic reactions with Fe(0), $FeCl_2$, pyrite and magnetite were assessed.
- Unlike at pH 12, at pH 7 only CT degradation by Fe(0) and pyrite was detected.
- Different C–Cl plots for CT hydrogenolysis and CT hydrolytic or thiolytic reduction.
- Reactions with Fe(0) and pyrite showed similar Λ for each compound regardless pH.

GRAPHICAL ABSTRACT

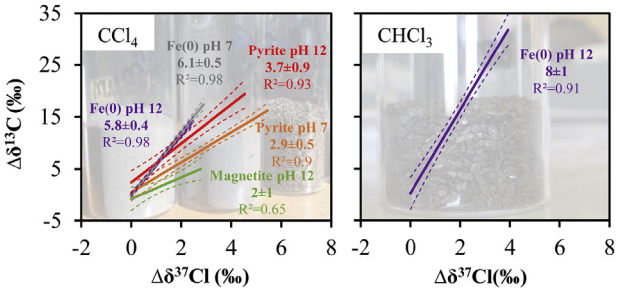

ARTICLE INFO

Article history:
Received 28 November 2017
Received in revised form
20 April 2018
Accepted 6 May 2018
Available online 7 May 2018

Handling Editor: Chang-Ping Yu

Keywords:
CSIA
Carbon tetrachloride
Chloroform
Pyrite
Fe(0)
Degradation pathways

ABSTRACT

A dual element C–Cl isotopic study was performed for assessing chlorinated methanes (CMs) abiotic transformation reactions mediated by iron minerals and Fe(0) to further distinguish them in natural attenuation monitoring or when applying remediation strategies in polluted sites. Isotope fractionation was investigated during carbon tetrachloride (CT) and chloroform (CF) degradation in anoxic batch experiments with Fe(0), with $FeCl_2$(aq), and with Fe-bearing minerals (magnetite, Mag and pyrite, Py) amended with $FeCl_2$(aq), at two different pH values (7 and 12) representative of field and remediation conditions. At pH 7, only CT batches with Fe(0) and Py underwent degradation and CF accumulation evidenced hydrogenolysis. With Py, thiolytic reduction was revealed by CS_2 yield and is a likely reason for different Λ value ($\Delta\delta^{13}C/\Delta\delta^{37}Cl$) comparing with Fe(0) experiments at pH 7 (2.9 ± 0.5 and 6.1 ± 0.5, respectively). At pH 12, all CT experiments showed degradation to CF, again with significant differences in Λ values between Fe(0) (5.8 ± 0.4) and Fe-bearing minerals (Mag, 2 ± 1, and Py, 3.7 ± 0.9), probably evidencing other parallel pathways (hydrolytic and thiolytic reduction). Variation of pH did not significantly affect the Λ values of CT degradation by Fe(0) nor Py.

CF degradation by Fe(0) at pH 12 showed a Λ (8 ± 1) similar to that reported at pH 7 (8 ± 2), suggesting CF hydrogenolysis as the main reaction and that CF alkaline hydrolysis (13.0 ± 0.8) was negligible.

* Corresponding author.
E-mail address: diana.rodriguez@ub.edu (D. Rodríguez-Fernández).

https://doi.org/10.1016/j.chemosphere.2018.05.036

Our data establish a base for discerning the predominant or combined pathways of CMs natural attenuation or for assessing the effectiveness of remediation strategies using recycled minerals or Fe(0).

1. Introduction

Chloroform (CF, $CHCl_3$) and carbon tetrachloride (CT, CCl_4) are chlorinated volatile organic compounds (VOCs) from the group of chlorinated methanes (CMs). Both are toxic and predicted to be carcinogenic substances (IARC, 1999). They are found in groundwater as a consequence of releases from chemical manufacturing processes or accidental spills (Zogorski et al., 2006), although CF can also be naturally formed (Cappelletti et al., 2012; Hunkeler et al., 2012; Breider et al., 2013).

Abiotic CMs degradation in groundwater mainly proceeds under anoxic conditions. The main CT degradation pathway is hydrogenolysis to CF, although CT reduction followed by hydrolytic or thiolytic substitution of dechlorinated intermediates to CO, CO_2 or CS_2 is also possible (He et al., 2015). Abiotic CF degradation processes under anoxic conditions include hydrogenolysis to DCM and reductive elimination to CH_4 (Song and Carraway, 2006; He et al., 2015). Bioremediation strategies for CMs are scarce (Penny et al., 2010; Cappelletti et al., 2012; Koenig et al., 2015). Thus, although both compounds can be biotically (Penny et al., 2010; Cappelletti et al., 2012) or abiotically degraded, they are considered recalcitrant compounds requiring targeted remediation strategies in groundwater.

In situ chemical oxidation is not an effective treatment for CT and CF due to the highly oxidized state of carbon (Huang et al., 2005; Huling and Pivetz, 2006). Alkaline hydrolysis (AH) has been studied for CF at laboratory and field scale as a new and effective remediation strategy (Torrentó et al., 2014) but CT hydrolysis is pH independent and extremely slow (Jeffers et al., 1989). Fortunately, zero-valent metals and Fe-bearing minerals have proven to mediate the transformation of CF and CT at laboratory scale (e.g. Matheson and Tratnyek, 1994; Támara and Butler, 2004; Feng and Lim, 2005; Zwank et al., 2005; He et al., 2015; Lee et al., 2015). Fe(0) has been commonly used in permeable reactive barriers (PRBs) since it is a strong reducing agent, cheaper and less harmful than other zero-valent metals (Vodyanitskii, 2014). Micro-sized Fe(0) has been used in long-functioning PRBs, while nano-sized Fe(0) injections have been recently used to renew PRBs in highly polluted sites (Obiri-Nyarko et al., 2014). Some minerals such as magnetite (Fe_3O_4, Mag hereafter) can be formed in Fe(0) PRBs reducing their efficiency (Vodyanitskii, 2014), while others, such as FeS, can promote CT degradation (Obiri-Nyarko et al., 2014). Since long-term evolution of PRBs is still not fully understood (Obiri-Nyarko et al., 2014) and Fe-bearing minerals such as pyrite (FeS_2, Py hereafter), green rusts or Mag are naturally ubiquitous in anoxic aquifers and/or in transition zones (Ferrey et al., 2004; Scheutz et al., 2011), it is interesting to assess their influence on CMs degradation.

Detection of CMs natural attenuation or monitoring of the above-mentioned remediation strategies can be challenging when relying on only by-products, since these daughter products can be further degraded, are difficult to quantify in the field (e.g. gases), could come from other parent compounds or stem from a secondary source (i.e. CF). In such cases, compound specific isotope analysis (CSIA) has been developed and matured into a widely applied method allowing the investigation of VOCs transformation reactions and the associated isotopic fractionation values (ε) (Renpenning and Nijenhuis, 2016). The occurrence of limiting steps prior to the reaction step that mask the real magnitude of the ε has been shown when mineral phases are involved in abiotic degradation processes (Elsner et al., 2007). Controlled laboratory studies are thus required to confine the ranges of possible ε values and determine conservative estimates of quantification of CMs degradation extent in the field. The concept of dual element (C–Cl) isotope plots featuring slopes ($\Lambda = \Delta\delta^{13}C/\Delta\delta^{37}Cl$) that are characteristic of different reaction mechanism, holds promise to provide information on the manner and order of chemical bond cleavage for organohalides (Nijenhuis et al., 2016) and this, in turn, may help to distinguish potential competing processes and to assess their individual effectiveness as field remediation strategies (Van Breukelen, 2007). Although some abiotic Λ values for CF were recently published (Heckel et al., 2017a; Torrentó et al., 2017), neither Λ for CT abiotic reactions nor field demonstrations are available.

In a multiple-compound polluted site in Òdena (Catalonia) (Palau et al., 2014), shifts in carbon isotopic composition of CF were attributed to AH (Torrentó et al., 2014) since alkaline conditions (pH ~12) were generated in recharge water concrete-based interception trenches. In contrast, detected shifts in the carbon isotopic composition of CT could not be explained by AH but here, reduction by Fe-bearing materials from the construction wastes used in the trenches could have played an important role (Torrentó et al., 2014). The presence of surficial iron patinas growths and of variable iron amounts in concrete-based aggregates obtained from one of the boreholes was confirmed by Scanning Electron Microscopy with X-ray microanalysis (SEM-EDS) and X-ray fluorescence (XRF) (data not published), but specific mineral phases are still under study.

In order to close this knowledge gap on isotopic data of abiotic CMs reactions and, therefore, to allow better field interpretations such as in the case of Òdena, this study aims at providing dual element isotope data on abiotic degradation of CT and CF by Fe(0) and Fe-bearing minerals with $FeCl_2$(aq) under anoxic conditions at pH 7 and 12. Characterization is based on monitoring the carbon and chloride isotopic composition ($\delta^{13}C$ and $\delta^{37}Cl$) of CF and CT, as well as on detecting volatile dissolved by-products to identify the existence of parallel reaction pathways. Nano-sized Fe(0) was used for CT experiments because it is more reactive than micro-sized Fe(0) (Song and Carraway, 2006). CF experiments at pH 12 were performed with milli-sized Fe(0) to compare the pH effect with published pH 7 experiments (Torrentó et al., 2017). Py and Mag were chosen as Fe-bearing minerals because they involve different potential redox species for reaction with CMs (Fe(II), and S_2^{2-} in Py, according to Kriegman-King and Reinhard (1994) and represent widespread oxidation products of Fe(0) in PRBs (He et al., 2015) and mining or industrial wastes, which are potential recyclable materials for remediation.

2. Materials and methods

2.1. Experimental setup

Experiments were prepared in an anaerobic chamber and performed in 42 mL VOA/EPA glass vials capped with PTFE-coated rubber stoppers and plastic screw caps. A summary of

experiment nomenclature, amendments and concentrations, incubation parameters representative of typical environmental conditions and performed analyses is provided in Table 1, together with data from already published CF experiments with milli-sized Fe(0) at pH 7 (Torrentó et al., 2017) for the sake of comparison. After the addition of the solid phase, vials were completely filled with buffered aqueous solution (at pH 7 or 12) without headspace, except for CT experiments with nano-sized Fe(0), for which the vials contained 21 mL liquid phase and 21 mL gas phase. For Mag and Py batches, $FeCl_2$(aq) was also added to the buffered solution to better mimic field conditions, and because it is thought that CT degradation reactions can be surface-mediated by Fe(II) sorbed to solid phases (Scherer et al., 1998; Amonette et al., 2000; Pecher et al., 2002; Elsner et al., 2004). Bottles with 0.6 mM of $FeCl_2$(aq) and without Fe-minerals (named as 'aq') were prepared as reactive controls for the potential of $FeCl_2$(aq) for CMs degradation. Controls (CO) with only buffered solution at the corresponding pH were prepared to observe losses or effects of the pH itself on CF transformation. The reaction started with the addition of pollutant pure phase to reach the initial theoretical concentration. Vials were placed in horizontal shakers at room temperature until sampling. Replicates (n vials) were prepared for each experiment and reaction vials were sacrificed at appropriate time intervals. The CT experiments with nano-sized Fe(0) were conducted in triplicate and headspace samples were taken from each single vial at appropriate time intervals. Concentration and C and Cl isotope ratios of parent compounds and potential by-products were monitored over time. The used analytical methods are included in Table 1.

Although Eh could not be monitored, it would be assumed below 0 V, postulated as the boundary for anoxic conditions (Morris et al., 2003; Hosono et al., 2011). At these Eh conditions, Fe(0) (and Py to a lesser extent) is not stable at pH 7 neither 12 (Fig. S1). Thermodynamically, Fe(0) oxidation should occur and electron release should be expected. More details about chemicals, minerals and Fe(0) preparation and characterization, sampling, samples preservation and analytical methods are available in the Supplementary Information (SI).

3. Results and discussion

In the following sections, isotope results for CF and CT degradation by the Fe(0), Mag, Py and $FeCl_2$(aq) are presented (Table 2)

Table 1
Summary of performed experiments nomenclature, conditions, procedure and analyses. The equipment used for each analysis is specified. n.u = not used in the experiment, n.a. = not analyzed.

Pollutant	pH	Name	Pollutant concentration (mM)	Fe(0)/ mineral loading (m^2/L)	$FeCl_2$ (mM)	*n* vials	Incubation temperature (°C)	Incubation time (days)	Shaker	By-products analyses	$\delta^{13}C$ analyses of parent compounds and by-products	$\delta^{37}Cl$ analyses of parent compounds	Ref.
CT	7	CT_Fe_7	2.6	28	n.u	1	25 ± 2	0.1	Horizontal[a] 300 rpm	VOCs HS-GC-qMS-1[d] as described in Heckel et al. (2017b)	HS-GC-IRMS-2[d] as described in Cretnik et al. (2013)	HS-GC-IRMS-2[d] as described in Heckel et al. (2017b)	This study
	12	CT_Fe_12				1	25 ± 2	0.1	Horizontal[a] 300 rpm				
	7	CT_aq_7	0.3	n.u	0.6	9	17.4 ± 0.3*	11	Horizontal[b] 100 rpm	VOCs, CS_2 HS-GC-MS[e] as described in Torrentó et al. (2017)	SPME-HS-GC-IRMS-1[e] as described in Martín-González et al. (2015)	HS-GC-qMS-2[f] as described in Heckel et al. (2017b) (n.a. for CT_Mag_7)	
	12	CT_aq_12				11	19.2 ± 0.4*	9					
						5	20 ± 2*	0.9					
	7	CT_Mag_7	0.3	17	0.6	20	15 ± 3*	11					
	12	CT_Mag_12			0.6	20	20 ± 2*	9					
	7	CT_Py_7	0.3	59	0.6	20	18.7 ± 0.3*	4					
	12	CT_Py_12			0.6	19	20 ± 1*	7					
						20	20.2 ± 0.1*	1					
CF	7	CF_CO_7	0.9	n.u.	n.u	6	25 ± 2	2	Horizontal[c] 200 rpm	VOCs HS-GC-TOF-MS[d] as described in Torrentó et al. (2017)	SPME-HS-GC-IRMS-1[e] as described in Martín-González et al. (2015)	HS-GC-IRMS-2[d] as described in Heckel et al. (2017b)	Torrentó et al. (2017)
	12	CF_CO_12	0.4	n.u	n.u	12	25 ± 2	9					This study
	7	CF_Fe_7	0.9	77	n.u	20	25 ± 2	2					Torrentó et al. (2017)
	12	CF_Fe_12	0.4			20	25 ± 2	9					This study
	7	CF_aq_7	0.4	n.u	0.6	9	17.4 ± 0.5*	8	Horizontal[b] 100 rpm	VOCs, CS_2 HS-GC-MS[e] as described in Torrentó et al. (2014)		HS-GC-qMS-2[f] as described in Heckel et al. (2017b)	
	12	CF_aq_12				10	17.2 ± 0.7*	23					
	7	CF_Mag_7	0.4	17	0.6	19	17.0 ± 0.5*	21				n.a.	
	12	CF_Mag_12				20	17.0 ± 0.6*	23					
	7	CF_Py_7	0.4	59	0.6	19	18 ± 1*	21				HS-GC-qMS-2[f] as described in Heckel et al. (2017b)	
	12	CF_Py_12				20	17.4 ± 0.5*	22				n.a.	

Equipment abbreviations correspond to headspace (HS)-gas chromatography (GC)- mass spectrometry (MS); HS-GC coupled to a time-of-flight (TOF) MS; GC quadrupole MS (GC-qMS); GC coupled to a isotope ratio mass spectrometer (GC-IRMS).
*Spot measurement when sampling.
[a] R1000 ROTH.
[b] Denlay Instruments LTD n° 941157.
[c] IKA KS 260 BASIC.
[d] In Institute of Groundwater Ecology of *Helmholtz Zentrum (München)*.
[e] In *Universitat de Barcelona*.
[f] In *Université de Neuchâtel*.

Table 2
Summary of isotope results, identified by-products and hypothesized degradation pathways. Uncertainty of Ɛ, AKIE and Λ ($\Delta\delta^{13}C/\Delta\delta^{37}Cl$) values corresponds to the 95% confidence intervals. AKIEs were calculated assuming C–Cl bond cleavage in the first rate-limiting reaction step. $AKIE_C$ values for CT and CF were calculated with z = x = n = 1 and $AKIE_{Cl}$ values with z = x = n = 4 for CT and of z = x = n = 3 for CF (Calculations in SI). Question marks indicate hypothesized pathways not proved in this research.

Experiment	By-products*	Ɛ (‰)	AKIE	Λ	Removal (%)	Proposed pathway
CT_Fe_7	CF	$\varepsilon C = -3.7 \pm 0.1$ $R^2 = 0.995$ $\varepsilon Cl = -0.58 \pm 0.04$ $R^2 = 0.98$	$AKIE_C = 1.0037 \pm 0.0001$ $AKIE_{Cl} = 1.00233 \pm 0.00004$	6.1 ± 0.5 $R^2 = 0.98$	99	Hydrogenolysis
CT_Fe_12	CF	$\varepsilon C = -3.4 \pm 0.1$ $R^2 = 0.993$ $\varepsilon Cl = -0.55 \pm 0.03$ $R^2 = 0.98$	$AKIE_C = 1.0034 \pm 0.0001$ $AKIE_{Cl} = 1.00220 \pm 0.00003$	5.8 ± 0.4 $R^2 = 0.98$	99	Hydrogenolysis
CT_aq_7	n.d.	no degradation				
CT_aq_12	CF	$\varepsilon C = -3 \pm 3$ $R^2 = 0.50$	$AKIE_C = 1.003 \pm 0.003$	High confidence interval	87	Hydrogenolysis
CT_Mag_7	n.d.	no degradation				
CT_Mag_12	CF	$\varepsilon C = -2 \pm 1$ $R^2 = 0.70$ $\varepsilon Cl = -0.8 \pm 0.2$ $R^2 = 0.93$	$AKIE_C = 1.002 \pm 0.001$ $AKIE_{Cl} = 1.0032 \pm 0.0002$	2 ± 1 $R^2 = 0.65$	98	Hydrogenolysis ± hydrolytic reduction?
CT_Py_7	CF, CS_2	$\varepsilon C = -5 \pm 2$ $R^2 = 0.70$ $\varepsilon Cl = -1.5 \pm 0.4$ $R^2 = 0.8$	$AKIE_C = 1.005 \pm 0.002$ $AKIE_{Cl} = 1.0060 \pm 0.0004$	2.9 ± 0.5 $R^2 = 0.9$	99	Hydrogenolysis and thiolytic reduction
CT_Py_12	CF, CS_2	$\varepsilon C = -4 \pm 1$ $R^2 = 0.87$ $\varepsilon Cl = -0.9 \pm 0.4$ $R^2 = 0.84$	$AKIE_C = 1.004 \pm 0.001$ $AKIE_{Cl} = 1.0036 \pm 0.0004$	3.7 ± 0.9 $R^2 = 0.93$	99	Hydrogenolysis and thiolytic reduction
CF_CO_7	n.d.	no degradation				
CF_CO_12	n.d.	n.c.	n.c			Partly by AH±reductive elimination?
CF_Fe_7[a]	DCM	$\varepsilon C = -33 \pm 11$ $R^2 = 0.82$ $\varepsilon Cl = -3 \pm 1$ $R^2 = 0.85$	$AKIE_C = 1.034 \pm 0.012$ $AKIE_{Cl} = 1.008 \pm 0.001$	8 ± 2 $R^2 = 0.93$	84	Hydrogenolysis ± reductive elimination?
CF_Fe_12	DCM	$\varepsilon C = -20 \pm 9$ $R^2 = 0.62$ $\varepsilon Cl = -2 \pm 1$ $R^2 = 0.64$	$AKIE_C = 1.020 \pm 0.009$ $AKIE_{Cl} = 1.006 \pm 0.001$	8 ± 1 $R^2 = 0.92$	85	Hydrogenolysis ± reductive elimination?
CF_aq_7	n.d.	no degradation				
CF_aq_12	n.d.	$\varepsilon C = -16 \pm 13$ $R^2 = 0.70$	$AKIE_C = 1.02 \pm 0.01$	$\delta^{37}Cl$ values n.a.	60	Partly by AH ± reductive elimination?
CF_Mag_7	n.d.	no degradation				
CF_Mag_12	n.d.	$\varepsilon C = -16 \pm 9$ $R^2 = 0.65$	$AKIE_C = 1.016 \pm 0.009$	$\delta^{37}Cl$ values n.a.	80	Partly by AH ± reductive elimination?
CF_Py_7	n.d.	no degradation				
CF_Py_12	DCM	$\varepsilon C = -20 \pm 7$ $R^2 = 0.85$	$AKIE_C = 1.020 \pm 0.007$	$\delta^{37}Cl$ values n.a.	62	Hydrogenolysis ± reductive elimination and partly by AH?

*Potential gas by-products such as CO, CO_2, CH_4 or formate were not analyzed. n.c. = not calculated, n.d. = not detected; n.a. = not analyzed.
[a] From Torrentó et al. (2017).

and compared with literature data. Concentrations were lower than expected in some experiments probably due to sorption on non-reactive sites of initial or newly formed solid phases as observed by other authors (Burris et al., 1995, 1998; Kim and Carraway, 2000; Song and Carraway, 2006). pH was constant for all experiments (SD < 0.5) except for CF_Mag_12, CF_Py_12, CT_aq_7, CT_Mag_7 (Fig. S2) where higher fluctuations might be attributable to iron corrosion processes and $Fe(OH)_3(am)$ formation.

3.1. Degradation study by Fe(0)

At both pH 7 and 12, CT concentration decrease below the detection limit in experiments with nano-sized Fe(0) was achieved before 4 h (Fig. 1A) and followed a pseudo-first-order kinetic law with rate constant values k_{SA} of $(4.9 \pm 0.6) \times 10^{-2}$ and $(4.4 \pm 0.1) \times 10^{-2}$ $Lm^{-2}h^{-1}$, respectively (Table S1). pH effect on k_{SA} was minimal as expected by thermodynamics, since E^0 of Fe(0) transformation to Fe(II) does not depend on pH.

Significant shifts in $\delta^{13}C_{CT}$ and $\delta^{37}Cl_{CT}$ were detected after 99.4% and 98.6% of CT removal at pH 7 and 12, respectively (Fig. 1B and C), resulting in very similar εC_{CT} (-3.7 ± 0.1, $R^2 = 0.995$ and -3.4 ± 0.1, $R^2 = 0.993$, respectively, see Eq. S4 and Fig. S3) and εCl_{CT} values (-0.58 ± 0.04, $R^2 = 0.98$ and -0.55 ± 0.03, $R^2 = 0.98$, respectively). Calculated $AKIE_C$ values (Eq. S5) were therefore also similar at pH 7 (1.0037 ± 0.0001) and 12 (1.0034 ± 0.0001) as for $AKIE_{Cl}$ values (1.0023 ± 0.0004 and 1.00220 ± 0.00003, respectively) (Table S2). These similarities regardless of pH confirmed that pH affects primarily intermediate [$\cdot CCl_3$] radical reactions rather than the initial rate-limiting step (Zwank et al., 2005). AKIEs values were below 50% of the Streitwieser limit for a C–Cl bond cleavage ($KIE_C = 1.057$, $KIE_{Cl} = 1.013$) (Elsner et al., 2005) and also below all reported values for abiotic and biotic reductive dechlorination of chlorinated compounds (Table S2), indicating significant mass transfer masking effects. CT is rapidly reduced when contacting a strong reducing agent like Fe(0) and, thus, the rate-limiting step of the reaction might be the diffusion of CT through the solution to the Fe(0) surface rather than the C–Cl bond cleavage (Arnold et al., 1999). In our experiments, this diffusion control could have been enhanced by the low concentration of CT (2.6 mM) compared to Fe(0) loading (28 m^2/L), but further research would be needed to confirm this hypothesis.

The use of HEPES in the pH 7 experiments might constrain exact

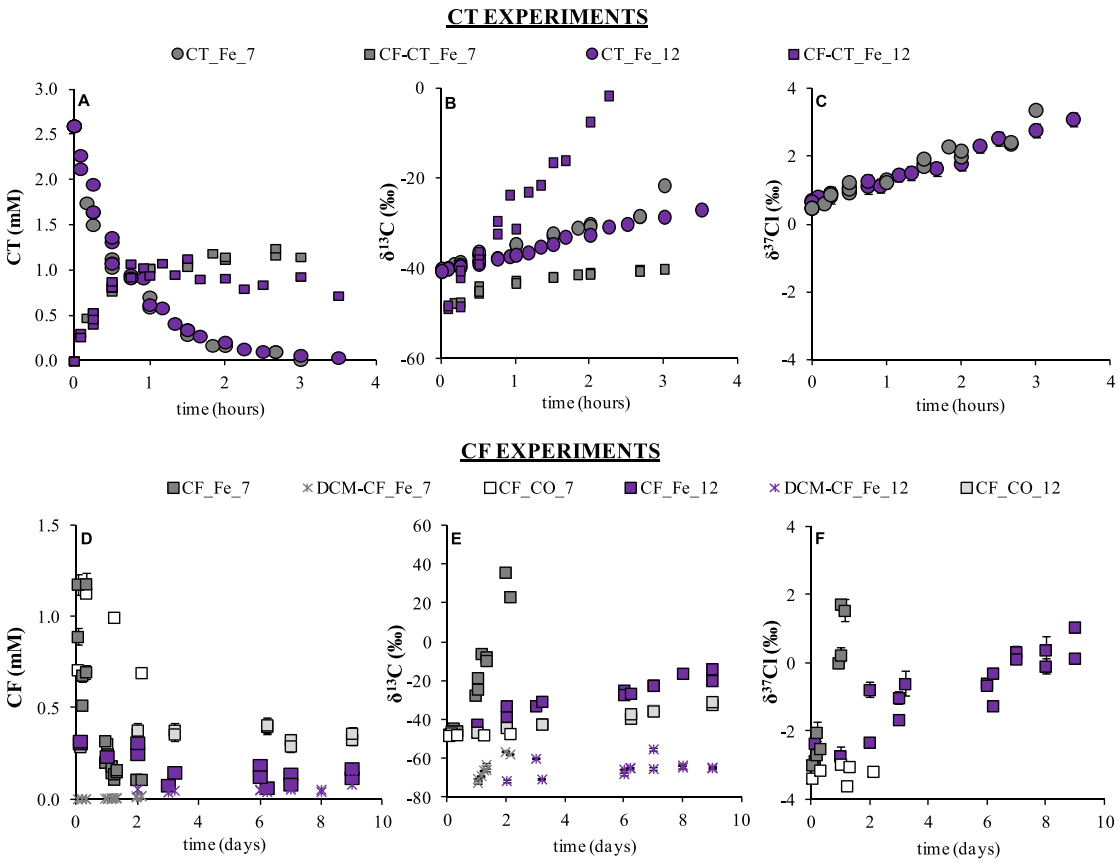

Fig. 1. Concentration (A, D), carbon (B, E) and chlorine (C, F) isotope composition ($\delta^{13}C$ and $\delta^{37}Cl$, ‰) over time in the CT (upper panels) and CF (lower panels) experiments at pH 7 and 12 with Fe(0) and control CF experiments (CO). CF_Fe_7 and CF_CO_7 data from Torrentó et al. (2017), and concentration and $\delta^{13}C$ evolution of CF and DCM as CT and CF by-products, respectively, are also shown. $\delta^{37}Cl$ data of by-products are not available. Error bars are smaller than symbols.

quantitative by-product distribution as it appears to alter by-product formation acting as possible H• radical donor and favoring CF formation (Elsner et al., 2004; Danielsen et al., 2005). However, by-product distribution study was not the aim of this work and by-products different from VOCs such as CH_4, CO, CO_2 (Lien and Zhang, 1999; Choe et al., 2001; Song and Carraway, 2006), were not analyzed. CF (45–56%) and DCM (up to 0.3% of initial CT) were detected as by-products at pH 7 and 12, after 99% of CT degradation, similarly to what was reported previously (Helland et al., 1995; Támara and Butler, 2004; Song and Carraway, 2006; Lien et al., 2007; Feng et al., 2008), which confirms CT and CF hydrogenolysis. Isotopic mass balances showed a maximum $\Delta\delta^{13}C_{SUM}$ (defined as final $\delta^{13}C_{SUM}$, Eq. S6, with respect to initial $\delta^{13}C_{SUM}$ considering, CT and by-product CF data) of only +1.5‰ at pH 7, compared to +35‰ at pH 12. Thus, at pH 7, CF degradation to other by-product different from DCM was insignificant in the present experimental conditions and duration (3.5 h). At pH 12, however, important further CF degradation (and a possible formation of other CT by-products) was evidenced by $\Delta\delta^{13}C_{SUM}$, $\Delta\delta^{13}C$ and more enriched $\delta^{13}C_{CF}$ values than those $\delta^{13}C_{CT}$ values of the parental CT (Fig. 1B).

As carbon and chlorine CT isotope fractionation is affected to the same extent by the above-mentioned masking effects, in a C–Cl dual plot these effects cancel out. As shown in Fig. 2A, Λ values obtained at pH 7 and 12 are similar (6.1 ± 0.5, $R^2 = 0.98$ and 5.8 ± 0.4, $R^2 = 0.98$, respectively), and indicative of CT hydrogenolysis attending to CF formation. The above-mentioned closed mass balances in CT_Fe_7 and the similar Λ at both pH revealed that CT hydrogenolysis by Fe(0) might also be the main pathway at pH 12. Moreover, if CT parallel pathways occur at pH 12, they should involve one C–Cl bond cleavage as hydrogenolysis does (Scheme S1). The obtained Λ values for CT degradation by Fe(0) show no statistically significant difference (with statistical significance at the $p < 0.05$ level, ANCOVA, $p = 0.8$) to that reported for biotically-mediated CT anaerobic degradation detected in field-derived microcosms (6.1 ± 0.5) (Rodríguez-Fernández et al., 2018).

The CF_Fe_12 experiments were carried out to complement existing data at pH 7 with milli-sized Fe(0) (Torrentó et al., 2017) (CF_Fe_7 in Table 1) and to provide, thereby, a more comprehensive picture of isotope effects in CF reduction by Fe(0). The corresponding control experiment without Fe(0) (CF_CO_12) showed certain variation in CF concentration (Fig. 1D) and although no VOCs by-products were detected, a significant $\delta^{13}C_{CF}$ shift of +17.6‰ was shown after 9 days (Fig. 1E). Since no isotopic changes occurred in previously reported CF_CO_7 (Torrentó et al., 2017), the results of CF_CO_12 experiment suggest that CF was degraded by AH. Assuming this was the only degradation fractionation process, the CF transformation extent by AH in CF_CO_12 was estimated to be $27 \pm 7\%$ using Eq. S7 and the ε_C of -57 ± 5‰ obtained by Torrentó et al. (2017). This extent of degradation fits well with the reported CF hydrolysis rates (Torrentó et al., 2014, 2017).

In the CF_Fe_12 experiment, CF degradation was also evidenced. CF concentration decreased with some fluctuations (Fig. 1D) causing poor correlation in rate constant k_{SA} ($(1.4 \pm 0.6) \times 10^{-3}$ $Lm^{-2}d^{-1}$, $R^2 = 0.67$, Table S1) and ε calculations ($\varepsilon C_{CF} = -20 \pm 9$ $R^2 = 0.62$ and $\varepsilon Cl_{CF} = -2 \pm 1$, $R^2 = 0.64$) (Fig. S4). Hence, comparison to CF_Fe_7 and literature data was based on evaluation of Λ values.

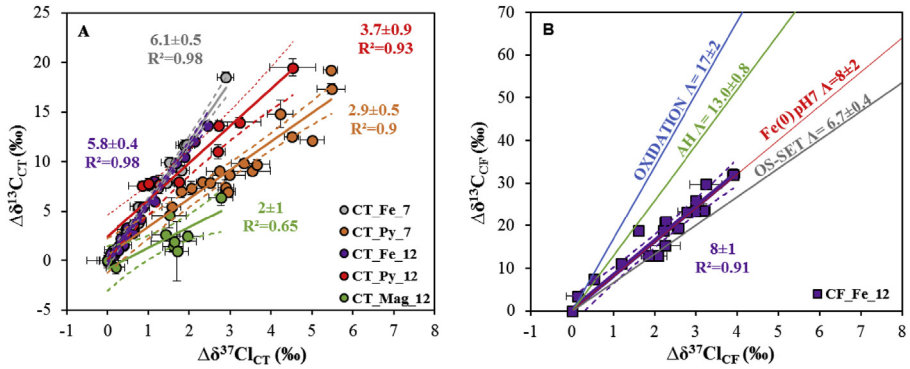

Fig. 2. Dual C–Cl isotope plot for CT (A) and CF (B) abiotic experiments. Same coloured solid and dashed lines correspond to linear regressions of the data sets of this study and 95% CI, respectively. Error bars show uncertainty in duplicate isotope measurements except for CT_Fe_7 and CT_Fe_12 experiments, where 0.5‰ and 0.2‰ were considered for $\delta^{13}C$ and $\delta^{37}Cl$, respectively. In some cases, error bars are smaller than symbols. Solid slopes in B correspond to CF abiotic degradation reference systems: oxidation by thermally-activated persulfate (blue), alkaline hydrolysis, AH (green), dechlorination by Fe(0) at pH 7 (red) (Torrentó et al., 2017) and reductive outer-sphere electron transfer by CO_2 radical anions, OS-SET (grey) (Heckel et al., 2017a). (For interpretation of the references to colour in this figure legend, the reader is referred to the Web version of this article.)

In this experiment, a moderated DCM accumulation was detected as by-product (≤0.3% yield after 9 days). This, together with the slower CF consumption in CF_Fe_12 compared to CF_Fe_7 (Fig. 1D), could be explained by Fe(0) surface passivation due to Fe-oxyhydroxides precipitation, enhanced at alkaline pH (Farrell et al., 2000; Támara and Butler, 2004). Low $\Delta\delta^{13}C_{DCM}$ was measured at pH 12 (+16‰ after 85% of CF removal) (Fig. 1E) similar to pH 7 (+15‰, after 87% of CF removal, Torrentó et al., 2017). The $\Delta\delta^{13}C_{SUM}$ (taking into account CF and DCM data) at pH 12 was only around +10‰, which might suggest an isotope-branching from CF or its intermediates (Zwank et al., 2005), that might have produced the low DCM carbon isotope fractionation observed for both pH.

The Λ value for CF_Fe_12 was 8 ± 1 ($R^2 = 0.91$), not significantly different from that of Torrentó et al. (2017) for CF_Fe_7 ($p = 0.05065$) (Fig. 2B). Combining the data at pH 7 and 12, the Λ value is not significantly different from that of CF reaction in model systems for outer-sphere single electron transfer (OS-SET) ($p = 0.1056$) (Heckel et al., 2017a), suggesting a concerted C–Cl bond cleavage, involving OS-SET in the first rate-limiting step. For CF-Fe_7, Torrentó et al. (2017) postulated two parallel CF dechlorination pathways (hydrogenolysis and reductive elimination) as reported for other CF reduction studies with micro-sized Fe(0) (Matheson and Tratnyek, 1994; Feng and Lim, 2005; Song and Carraway, 2006). In the present experiments, CF reductive elimination related by-products (e.g. CH_4, CO and $HCOO^-$) were not analyzed, and thus, further conclusions are limited. The similar Λ values for Fe(0) are far from the Λ = 13.0 ± 0.8 for CF AH (Torrentó et al., 2017), indicating that AH in CF_Fe_12 was negligible. Accordingly, negligible contribution of AH was evidenced by assessing the distribution (F) of AH and dechlorination by Fe(0) to the total CF degradation following Van Breukelen (2007) and using Eq (S8) and Ɛ data from Torrentó et al. (2017).

3.2. Degradation study by $FeCl_2$(aq) and Mag

Despite concentration fluctuations (Fig. 3A), no significant $\delta^{13}C_{CT}$ shifts over time were observed in the CT_aq_7 and CT_Mag_7 experiments (−41.9 ± 0.5‰, n = 9 and −41.4 ± 0.5‰, n = 6, respectively, Fig. 3B) and no VOCs by-products were detected. CT degradation therefore does not seem to occur in these experiments. In fact, the analogous experiments with CF at pH 7 neither showed also significant changes in $\delta^{13}C_{CF}$ (−49.2 ± 0.2‰, n = 5, and −49.0 ± 0.6‰, n = 7, for CF_Mag_7 and CF_aq_7 experiments, respectively) (Fig. 3B). This agrees with the decrease in the degradation efficiency of aged Fe(0) PRBs when Mag is formed through corrosion (Vodyanitskii, 2014). However, CT degradation by Mag has been previously reported in the literature under different experimental conditions (Zwank et al., 2005; Hanoch et al., 2006; Maithreepala and Doong, 2007; Vikesland et al., 2007). Further discussion about this discrepancy can be found in the SI.

In contrast, at pH 12, CT degradation occurred and kinetics of CT_Mag_12 and CT_aq_12 followed a pseudo-first-order rate law with a k_{SA} of $(8 \pm 5) \times 10^{-2} Lm^{-2}d^{-1}$ and k' of 0.3 ± 0.2 d^{-1}, respectively (Table S3). CT degradation was confirmed by significant $\Delta\delta^{13}C_{CT}$ (Fig. 3E) and $\Delta\delta^{37}Cl_{CT}$ (Fig. 3F) after 87 and 98% CT removal in the CT_aq_12 and CT_Mag_12 experiments, respectively, obtaining $\varepsilon C_{CT} = -2 \pm 1‰$ ($R^2 = 0.7$) and $\varepsilon Cl_{CT} = -0.8 \pm 0.2‰$ ($R^2 = 0.93$) for CT_Mag_12 (Fig. S6) and $\varepsilon C_{CT} = -2 \pm 3‰$ for CT_aq_12, but with poor linear regression ($R^2 = 0.5$) (Fig. S7). $AKIE_C$ (1.002 ± 0.0001) and $AKIE_{Cl}$ (1.0032 ± 0.0002) values of CT_Mag_12 were well below 50% of the Streitwieser limit for a C–Cl bond cleavage (Elsner et al., 2005) and also below the reported values for abiotic and biotic reductive dechlorination of chlorinated compounds (Table S2), suggesting significant mass transfer masking effects as for Fe(0). A maximum CF yield of +38% and +26% in CT_Mag_12 and CT_aq_12, respectively (Fig. S5), evidenced CT hydrogenolysis. $\delta^{13}C$ enrichment in the produced CF was detected. To further study CF degradation, analogous experiments with CF at pH 12 were performed and showed a CF concentration decrease to values down to 0.2–0.1 mM after 23 days (Fig. 3D). Obtained pseudo-first-order rate constants had poor correlation (k'=(6 ± 3) × 10^{-2} d^{-1}, $R^2 = 0.6$, for CF_aq_12 and k_{SA}=(6 ± 2) × 10^{-3} $Lm^{-2}d^{-1}$, $R^2 = 0.7$, for CF_Mag_12, Table S3). In both experiments at pH 12, degradation was confirmed by $\delta^{13}C$ shifts (Fig. 3E). Comparing with the absence of CF degradation in the pH 7 analogous experiments, AH could be assumed as the main degradation pathway in these experiments (Torrentó et al., 2017). However, despite poor regression, the obtained values of εC_{CF} for CF_Mag_12 (−16 ± 9‰, $R^2 = 0.65$) and CF_aq_12 (−16 ± 13‰, $R^2 = 0.70$) (Fig. S6, S7) are in the range for CF reductive dechlorination studies (Table S2) and far away from the reported values for CF AH at pH 12 (−57 ± 5‰) (Torrentó et al., 2017). These results suggest the occurrence of additional parallel pathways (such as CF reductive elimination to CH_4) (Scheme S1). Since nor CF Cl isotope ratios neither other non-chlorinated potential by-products were measured in these experiments, further conclusions cannot be drawn.

The calculated Λ value for CT_aq_12 (2 ± 3, $R^2 = 0.67$) was discarded due to its wide confidence interval, while that for CT_Mag_12 (2 ± 1, $R^2 = 0.65$) (Fig. 2A) was, despite its poor linear

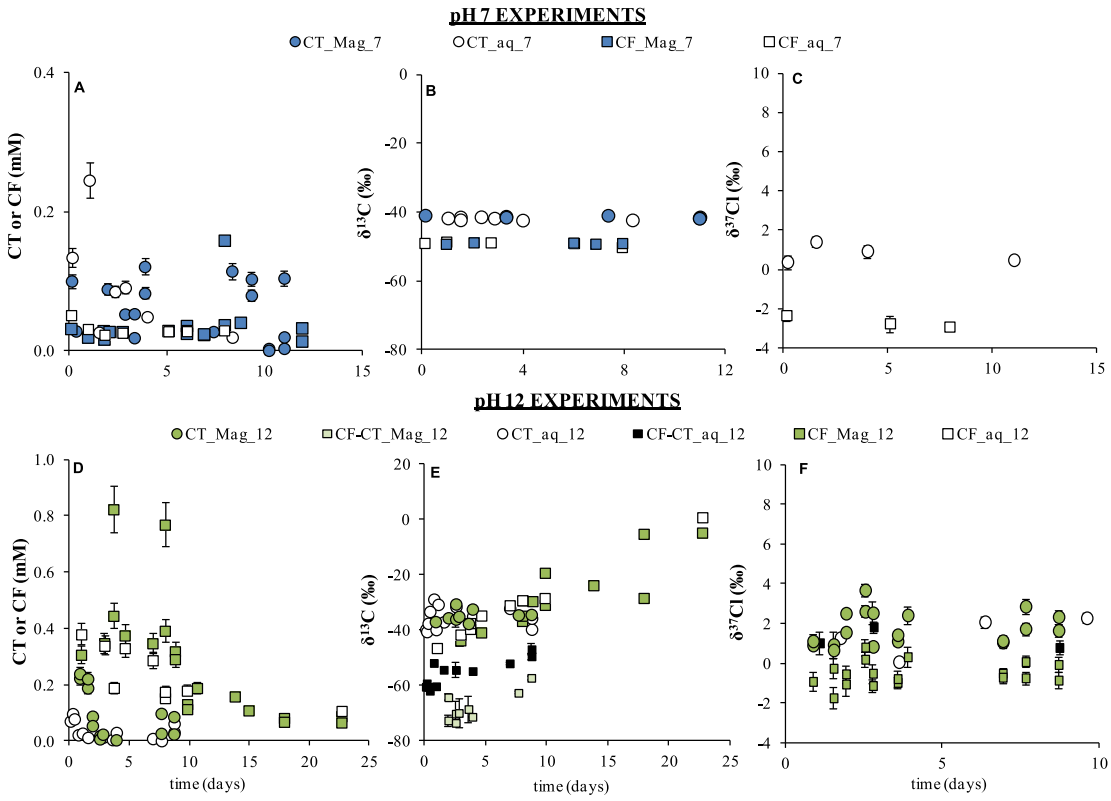

Fig. 3. Concentration (A, D) and carbon (B, E) and chlorine (C, F) isotope composition ($\delta^{13}C$ and $\delta^{37}Cl$, ‰) over time in the CT and CF experiments at pH 7 (upper panels) and 12 (lower panels) with magnetite and $FeCl_2$(aq)(Mag) and $FeCl_2$(aq)alone (aq). Isotope data of by-products of each experiment are also shown and named as 'by-product-experiment name' to distinguish them from experiments where those compounds are parental compounds. In some cases, error bars are smaller than symbols.

regression, highly statistically different ($p < 0.0001$) from those of CT_Fe_7 and CT_Fe_12. It suggests that although CF was formed as by-product in both Fe(0) and Mag CT experiments, parallel pathways other than hydrogenolysis could have occurred in CT_Mag_12. Also, a different first rate-determining step between reactions such as that producing CF or CO (hypothesized by-product by CT hydrolytic reduction according to Danielsen and Hayes (2004) might have occurred. That case would question whether branching in trichloromethyl free radical [$\cdot CCl_3$] or thrichlorocarbanion [$:CCl_3^-$] intermediates (Scheme S1) were responsible for by-products distribution (Danielsen and Hayes, 2004; Elsner et al., 2004; Zwank et al., 2005) because intermediates branching alone would have not affected CT isotope fractionation and Λ would have been similar. Differences in Λ value might be also explained by a change in transition states in mineral surfaces (Elsner et al., 2004).

The absence of CT degradation at pH 7 compared to pH 12, might be attributed to the control that pH exerts on Mag reactivity (see SI for further discussion). Under our experimental conditions, CT degradation by $FeCl_2$(aq) and Mag was only feasible under alkaline conditions. Although further field research would be required, Mag might be responsible of $\delta^{13}C_{CT}$ fractionation detected in the alkaline trenches of the Òdena field site (Torrentó et al., 2014) given that Mag is an ubiquitous mineral, commonly present in construction wastes.

3.3. Degradation study by Py

CT concentrations in CT_Py_7 and CT_Py_12 decreased quickly, especially at pH 12 where they reached 0.01 mM after 4 h (Fig. 4A, D). Although poor correlated, degradation followed a pseudo-first-order rate law for CT_Py_7 ($k_{SA}=(1.6 \pm 0.6) \times 10^{-2}$ $Lm^{-2}d^{-1}$, $R^2 = 0.72$) and CT_Py_12 ($(2 \pm 1) \times 10^{-2}$ $Lm^{-2}d^{-1}$, $R^2 = 0.6$), (Table S3). CT degradation was confirmed at both pH by enrichment in ^{13}C and ^{37}Cl (Fig. 4). Calculated εC_{CT} and εCl_{CT} values were -5 ± 2‰ ($R^2 = 0.7$) and -1.5 ± 0.4‰ ($R^2 = 0.8$), respectively for CT_Py_7 (Fig. S8), and -4 ± 1‰ ($R^2 = 0.87$) and -0.9 ± 0.4‰ ($R^2 = 0.84$), respectively for CT_Py_12 (Fig. S9). Corresponding $AKIE_C$ (1.005 ± 0.002 and 1.004 ± 0.001, respectively) and $AKIE_{Cl}$ values (1.0060 ± 0.0004 and 1.0036 ± 0.0004, respectively) indicate significant mass transfer masking effects for the same reasons than for Fe(0) and Mag experiments. Poor correlation in CT_Py_7 might be linked to the low pH reached (4.7 ± 1.1, Fig. S2) that might have caused changes in Py surface (Bonnissel-Gissinger et al., 1998) affecting CT degradation.

In both experiments, the formation of by-products CF and CS_2 was observed (Fig. S5) agreeing with literature (Kriegman-King and Reinhard, 1994; Devlin and Muller, 1999). Analogous experiments with Py and CF as parent compound demonstrated no CF degradation at pH 7 ($\delta^{13}C_{CF} = -49.1 \pm 0.3$‰, $\delta^{37}Cl_{CF} = -3.1 \pm 0.3$‰, $n = 7$). At pH 12, however, CF degradation was evidenced by a clear CF concentration decrease ($k_{SA}=(2 \pm 1) \times 10^{-2}$ $Lm^{-2}d^{-1}$, $R^2 = 0.6$), a significant carbon isotope enrichment ($\varepsilon C_{CF} = -20 \pm 7$‰, $R^2 = 0.85$) (Fig. S9) and up to a 6% DCM yield (Fig. S5). Py oxidation at pH 12 by CF is an unknown process but, by analogy to CT (Kriegman-King and Reinhard, 1992, 1994), it would follow Eq. (1), with an overall reaction potential higher at pH 12 (0.7 V) than at pH 7 (0.5 V).

$$FeS_2 + CHCl_3 + 8H_2O \rightarrow Fe^{2+} + 2SO_4^{2-} + CH_2Cl_2 + Cl^- + 15H^+ + 12e^- \quad (1)$$

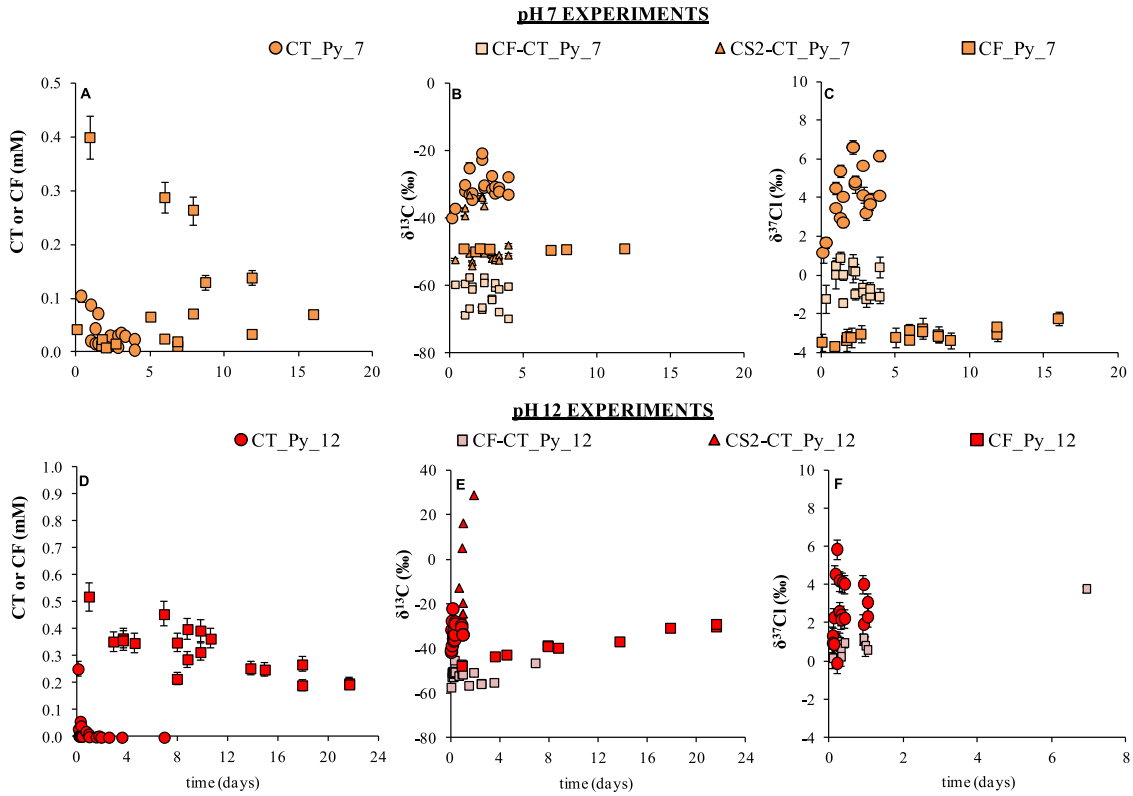

Fig. 4. Concentration (A, D) and carbon (B, E) and chlorine (C, F) isotope composition ($\delta^{13}C$ and $\delta^{37}Cl$, ‰) over time in the CT and CF experiments at pH 7 (upper panels) and 12 (lower panels) with pyrite (Py) and $FeCl_2$(aq). Isotope data of by-products of each experiment are also shown and named as 'by-product-experiment name' to distinguish them from experiments where those compounds are parental compounds. In some cases, error bars are smaller than symbols.

The accumulation of DCM (Fig. S5) suggests that hydrogenolysis together with AH might be responsible for CF carbon isotope fractionation. Since $\delta^{37}Cl$ was not measured in this experiment, quantification of each pathway following Eq. (S8) is not possible.

The detected CS_2 in the CT experiments with Py (Fig. S5) may form via aqueous or adsorbed HS^- (Kriegman-King and Reinhard, 1992) or via S_2^{2-} sites on Py surface acting as electron donor (Kriegman-King and Reinhard, 1994). Despite fluctuations, shifts in $\delta^{13}C_{CS2}$ values (Fig. 4B) and non-closed isotopic mass balance calculations at pH 7 ($\delta^{13}C_{SUM}$ range from −44 to −59‰) might reveal further CS_2 degradation since, as mentioned above, these shifts in $\delta^{13}C_{SUM}$ cannot be attributed to CF degradation. At pH 12, CS_2 degradation was confirmed by the much enriched $\delta^{13}C_{CS2}$ values (+28.8‰) with respect to the initial $\delta^{13}C_{CT}$ after 46 h (Fig. 4E). CS_2 degradation might occur through hydrolysis mediated by hydroxide ions at these alkaline conditions (11.8 ± 0.2). CS_2 alkaline hydrolysis has been proven at laboratory scale (Svoronos and Bruno, 2002) with rate constants at 25 °C ranging between 10^{-4} and $10^{-3}\ M^{-1}s^{-1}$, equivalent to half-lifes of 1–13 days at pH 11.8. According to literature (Peyton et al., 1976; Adewuyi and Carmichael, 1987; Kriegman-King and Reinhard, 1992, 1994; McGeough et al., 2007), CS_2 is stable to hydrolysis within the pH range of 4–10, suggesting Py mediation in the potentially occurring CS_2 degradation at pH 7, as Fe(0) involvement has also been reported (McGeough et al., 2007). Further research is needed to clarify this point. In any case, it follows that the previously proposed CF:CS_2 mass ratio for distinguishing CT transformations reactions (Devlin and Muller, 1999; Davis et al., 2003) is inappropriate.

The obtained Λ values for CT_Py_7 (2.9 ± 0.5, $R^2 = 0.9$) and CT_Py_12 experiments (3.7 ± 0.9, $R^2 = 0.93$) are similar to each other and to that of CT_Mag_12 ($p = 0.2302$), but they are statistically different from that of CT hydrogenolysis by Fe(0) experiments at both pH values ($p < 0.0001$) (Fig. 2A). CT thiolytic reduction evidenced by CS_2 formation is thus supported by means of C–Cl Λ. Moreover, since the obtained Λ values in CT_Mag_12 and in CT experiments with Py were similar, a comparable contribution of initial parallel reaction mechanisms for both reactions is hypothesized (hydrolytic and thiolytic reduction, respectively Scheme S1).

4. Conclusions

CT and CF degradation by Fe(0) occurs at pH 7 and 12, with similar C–Cl Λ values at both pH values for each compound (8 ± 2 and 8 ± 1 for CF; 6.1 ± 0.5 and 5.8 ± 0.4 for CT, respectively), pointing in both cases to a hydrogenolysis pathway. Accumulation of recalcitrant DCM in this pathway should be taken into consideration in remediation strategies by PRBs.

Isotope fractionation proved that under our experimental conditions, $FeCl_2$(aq), Mag and Py are effective reducing agents for CT at pH 12, whereas at pH 7 only Py was able to degrade CT. CF was detected as by-product in all CT-degrading experiments, while CS_2 was only detected with Py. The occurrence of parallel CT hydrogenolysis and hydrolytic or thiolytic reduction pathways was also evidenced by the dual-plot approach, showing CT experiments with $FeCl_2$(aq) and Mag at pH 12 (2 ± 1) and with Py (2.9 ± 0.5 and 3.7 ± 0.9 at pH 7 and 12) Λ values different than that for hydrogenolysis alone with Fe(0) (6.1 ± 0.5 at pH 7). Further CF and CS_2 degradation at pH 12 was confirmed through isotopic tracking, reaffirming that by-products are not always traceable to confirm parent compound degradation. Mag and Py are thus effective minerals for abiotic CT remediation strategies, especially under

alkaline conditions, where the accumulation of harmful by-products is avoided by further degradation. On the contrary, under aquifer conditions, recycling these minerals for cost-effective PRB-building requires ensuring subsequent CF and CS_2 elimination. The studied CMs degradation reactions might be diffusion-controlled under natural field conditions, as it was previously reported (Elsner et al., 2007; Thullner et al., 2013). Thus, due to this isotope masking by rate-limitations in mass transfer, the highest reported ε value should be used for a conservative assessment of CMs degradation extent (Elsner, 2010; Thullner et al., 2012). However, if these minerals or Fe(0) were used as remediation techniques, where a high contaminant/mineral ratio is normally used, the C–Cl bond cleavage might be the rate-limiting step. Nevertheless, further research would be needed to confirm this hypothesis.

To sum up, all the data provided in this dual element C–Cl isotopic approach – especially first-time-published abiotic CT Λ values – in combination with earlier data for CF abiotic (Heckel et al., 2017a; Torrentó et al., 2017) and CT and CF biotic transformation reactions (Rodríguez-Fernández et al., 2018), improve considerably the isotopic database of CMs reactions. This information could be further applied in field studies for discerning the predominant pathway or the contribution of combined pathways in CMs natural attenuation following Van Breukelen (2007) or assessing the effect of remediation treatments over time.

Acknowledgements

This research was supported by a Marie Curie Career Integration Grant in the framework of IMOTEC-BOX project (PCIG9-GA-2011-293808), REMEDIATION (CGL2014-57215-C4-1-R) and PACE (CGL2017-87216-C4-1-R) both projects from Spanish Ministry of Economy and AEI/FEDER, UE; as well as the Catalan Government 2017SGR 1733 project. We thank technical support from CCiT-UB and the work of the undergraduate students D.García and F.Bagaria. D.Rodríguez-Fernández acknowledges FPU2012/01615 and Beca Fundació Pedro i Pons 2014 and M. Rosell, Ramón y Cajal contract (RYC-2012-11920). We thank the editor and the anonymous reviewers for comments that improved the quality of the manuscript.

Appendix A. Supplementary data

Supplementary data related to this article can be found at https://doi.org/10.1016/j.chemosphere.2018.05.036.

References

Adewuyi, Y.G., Carmichael, G.R., 1987. Kinetics of hydrolysis and oxidation of carbon disulfide by hydrogen peroxide in alkaline medium and application to carbonyl sulfide. Environ. Sci. Technol. 21, 170–177. https://doi.org/10.1021/es00156a602.

Amonette, J.E., Workman, D.J., Kennedy, D.W., Fruchter, J.S., Gorby, Y.A., 2000. Dechlorination of carbon tetrachloride by Fe (II) associated with goethite. Environ. Sci. Technol. 34, 4606–4613. https://doi.org/10.1021/es9913582.

Arnold, W.A., Ball, W.P., Roberts, A.L., 1999. Polychlorinated ethane reaction with zero-valent zinc: pathways and rate control. J. Contam. Hydrol. 40, 183–200. https://doi.org/10.1016/S0169-7722(99)00045-5.

Bonnissel-Gissinger, P., Alnot, M., Ehrhardt, J.J., Behra, P., 1998. Surface oxidation of pyrite as a function of pH. Environ. Sci. Technol. 32, 2839–2845. https://doi.org/10.1021/es980213c.

Breider, F., Albers, C.N., Hunkeler, D., 2013. Assessing the role of trichloroacetyl-containing compounds in the natural formation of chloroform using stable carbon isotopes analysis. Chemosphere 90, 441–448. https://doi.org/10.1016/j.chemosphere.2012.07.058.

Burris, D.R., Campbell, T.J., Manoranjan, V.S., 1995. Sorption of trichloroethylene and tetrachloroethylene in a batch reactive metallic iron-water system. Environ. Sci. Technol. 29, 2850–2855. https://doi.org/10.1021/es00011a022.

Burris, D.R., Allen-King, R.M., Manoranjan, V.S., Campbell, T.J., Loraine, G.A., Deng, B., 1998. Chlorinated ethene reduction by cast iron: sorption and mass transfer. J. Environ. Eng. 124, 1012–1019. https://doi.org/10.1061/(ASCE)0733-9372(1998)124:10(1012).

Cappelletti, M., Frascari, D., Zannoni, D., Fedi, S., 2012. Microbial degradation of chloroform. Appl. Microbiol. Biotechnol. 96, 1395–1409. https://doi.org/10.1007/s00253-012-4494-1.

Choe, S., Lee, S.H., Chang, Y.Y., Hwang, K.Y., Khim, J., 2001. Rapid reductive destruction of hazardous organic compounds by nanoscale Fe^0. Chemosphere 42, 367–372. https://doi.org/10.1016/S0045-6535(00)00147-8.

Cretnik, S., Thoreson, K.A., Bernstein, A., Ebert, K., Buchner, D., Laskov, C., Haderlein, S., Shouakar-stash, O., Kliegman, S., McNeill, K., Elsner, M., 2013. Reductive dechlorination of TCE by chemical model systems in comparison to dehalogenating bacteria: insights from dual element isotope analysis ($^{13}C/^{12}C$, $^{37}Cl/^{35}Cl$). Environ. Sci. Technol. 47, 6855–6863. https://doi.org/10.1021/es400107n.

Danielsen, K.M., Hayes, K.F., 2004. pH dependence of carbon tetrachloride reductive dechlorination by magnetite. Environ. Sci. Technol. 38, 4745–4752. https://doi.org/10.1021/es0496874.

Danielsen, K.M., Gland, J.L., Hayes, K.F., 2005. Influence of amine buffers on carbon tetrachloride reductive dechlorination by the iron oxide magnetite. Environ. Sci. Technol. 39, 756–763. https://doi.org/10.1021/es049635e.

Davis, A., Fennemore, G.G., Peck, C., Walker, C.R., McIlwraith, J., Thomas, S., 2003. Degradation of carbon tetrachloride in a reducing groundwater environment: implications for natural attenuation. Appl. Geochem. 18, 503–525. https://doi.org/10.1016/S0883-2927(02)00102-6.

Devlin, J.F., Muller, D., 1999. Field and laboratory studies of carbon tetrachloride transformation in a sandy aquifer under sulfate reducing conditions. Environ. Sci. Technol. 33, 1021–1027. https://doi.org/10.1021/es9806884.

Elsner, M., Haderlein, S.B., Kellerhals, T., Luzi, S., Zwank, L., Angst, W., Schwarzenbach, R.P., 2004. Mechanisms and products of surface-mediated reductive dehalogenation of carbon tetrachloride by Fe(II) on goethite. Environ. Sci. Technol. 38, 2058–2066. https://doi.org/10.1021/es034741m.

Elsner, M., Zwank, L., Hunkeler, D., Schwarzenbach, R.P., 2005. A new concept linking observable stable isotope fractionation to transformation pathways of organic pollutants. Environ. Sci. Technol. 39, 6896–6916. https://doi.org/10.1021/es0504587.

Elsner, M., Cwiertny, D.M., Roberts, A.L., Sherwood Lollar, B., 2007. 1,1,2,2-Tetrachloroethane reactions with OH^-, Cr(II), granular iron, and a copper - iron bimetal: insights from product formation and associated carbon isotope fractionation. Environ. Sci. Technol. 41, 4111–4117. https://doi.org/10.1021/es072046z.

Elsner, M., 2010. Stable isotope fractionation to investigate natural transformation mechanisms of organic contaminants: principles, prospects and limitations. J. Environ. Monit. 12, 2005–2031. https://doi.org/10.1039/c0em00277a.

Farrell, J., Kason, M., Melitas, N., Li, T., 2000. Investigation of the long-term performance of zero-valent iron for reductive dechlorination of trichloroethylene. Environ. Sci. Technol. 34, 514–521. https://doi.org/10.1021/es990716y.

Feng, J., Lim, T.T., 2005. Pathways and kinetics of carbon tetrachloride and chloroform reductions by nano-scale Fe and Fe/Ni particles: comparison with commercial micro-scale Fe and Zn. Chemosphere 59, 1267–1277. https://doi.org/10.1016/j.chemosphere.2004.11.038.

Feng, J., Zhu, B.-W., Lim, T.T., 2008. Reduction of chlorinated methanes with nano-scale Fe particles: effects of amphiphiles on the dechlorination reaction and two-parameter regression for kinetic prediction. Chemosphere 73, 1817–1823. https://doi.org/10.1016/j.chemosphere.2008.08.014.

Ferrey, M.L., Wilkin, R.T., Ford, R.G., Wilson, J.T., 2004. Nonbiological removal of cis-dichloroethylene and 1,1-dichloroethylene in aquifer sediment containing magnetite. Environ. Sci. Technol. 38, 1746–1752. https://doi.org/10.1021/es0305609.

Hanoch, R.J., Shao, H., Butler, E.C., 2006. Transformation of carbon tetrachloride by bisulfide treated goethite, hematite, magnetite, and kaolinite. Chemosphere 63, 323–334. https://doi.org/10.1016/j.chemosphere.2005.07.016.

He, Y.T., Wilson, J.T., Su, C., Wilkin, R.T., 2015. Review of abiotic degradation of chlorinated solvents by reactive iron minerals in aquifers. Groundw. Monit. Remed. 35, 57–75. https://doi.org/10.1111/gwmr.12111.

Heckel, B., Cretnik, S., Kliegman, S., Shouakar-Stash, O., McNeill, K., Elsner, M., 2017a. Reductive outer-sphere single electron transfer is an exception rather than the rule in natural and engineered chlorinated ethene dehalogenation. Environ. Sci. Technol. 51, 9663–9673. https://doi.org/10.1021/acs.est.7b01447.

Heckel, B., Rodríguez-Fernández, D., Torrentó, C., Meyer, A., Palau, J., Domènech, C., Rosell, M., Soler, A., Hunkeler, D., Elsner, M., 2017b. Compound-specific chlorine isotope analysis of tetrachloromethane and trichloromethane by gas chromatography-isotope ratio mass spectrometry vs gas chromatography-quadrupole mass spectrometry: method development and evaluation of precision and trueness. Anal. Chem. 89, 3411–3420. https://doi.org/10.1021/acs.analchem.6b04129.

Helland, B.R., Alvarez, P.J.J., Schnoor, J.L., 1995. Reductive dechlorination of carbon tetrachloride with elemental iron. J. Hazard Mater. 41, 205–216. https://doi.org/10.1016/0304-3894(94)00111-S.

Hosono, T., Nakano, T., Shimizu, Y., Onodera, S. ichi, Taniguchi, M., 2011. Hydrogeological constraint on nitrate and arsenic contamination in Asian metropolitan groundwater. Hydrol. Process. 25, 2742–2754. https://doi.org/10.1002/hyp.8015.

Huang, K.C., Zhao, Z., Hoag, G.E., Dahmani, A., Block, P.A., 2005. Degradation of volatile organic compounds with thermally activated persulfate oxidation. Chemosphere 61, 551–560. https://doi.org/10.1016/j.chemosphere.2005.02.032.

Huling, S.G., Pivetz, B.E., 2006. In-situ Chemical Oxidation-engineering Issue. EPA/

600/R-06/072. U.S. Environmental Protection Agency Office of Research and Development, National Risk Management Research Laboratory, Cincinnati, OH.
Hunkeler, D., Laier, T., Breider, F., Jacobsen, O.S., 2012. Demonstrating a natural origin of chloroform in groundwater using stable carbon isotopes. Environ. Sci. Technol. 46, 6096–6101. https://doi.org/10.1021/es204585d.
IARC, 1999. IARC Monographs on the Evaluation of Carcinogenic Risks to Humans, vol. 71, pp. 319–335.
Jeffers, P.M., Ward, L.M., Woytowltch, L.M., Wolfe, N.L., 1989. Homogeneous hydrolysis rate constants for selected chlorinated methanes, ethanes, ethenes, and propanes. Environ. Sci. Technol. 23, 965–969. https://doi.org/10.1021/es00066a006.
Kim, Y.H., Carraway, E.R., 2000. Dechlorination of pentachlorophenol by zero valent iron and modified zero valent irons. Environ. Sci. Technol. 34, 2014–2017. https://doi.org/10.1021/es991129f.
Koenig, J., Lee, M., Manefield, M., 2015. Aliphatic organochlorine degradation in subsurface environments. Rev. Environ. Sci. Bio/Technol. 14, 49–71. https://doi.org/10.1007/s11157-014-9345-3.
Kriegman-King, M.R., Reinhard, M., 1992. Transformation of carbon tetrachloride in the presence of sulfide, biotite, and vermiculite. Environ. Sci. Technol. 26, 2198–2206. https://doi.org/10.1021/es00035a019.
Kriegman-King, M.R., Reinhard, M., 1994. Transformation of carbon tetrachloride by pyrite in aqueous solution. Environ. Sci. Technol. 28, 692–700. https://doi.org/10.1021/es00053a025.
Lee, M., Wells, E., Wong, Y.K., Koenig, J., Adrian, L., Richnow, H.H., Manefield, M., 2015. Relative contributions of Dehalobacter and zerovalent iron in the degradation of chlorinated methanes. Environ. Sci. Technol. 49, 4481–4489. https://doi.org/10.1021/es5052364.
Lien, H.L., Zhang, W.X., 1999. Transformation of chlorinated methanes by nanoscale iron particles. J. Environ. Eng. 125, 1042–1047. https://doi.org/10.1061/(ASCE)0733-9372(1999)125:11(1042).
Lien, H.-L., Jhuo, Y.-S., Chen, L.-H., 2007. Effect of heavy metals on dechlorination of carbon tetrachloride by iron nanoparticles. Environ. Eng. Sci. 24, 21–30. https://doi.org/10.1089/ees.2007.24.21.
Maithreepala, R.A., Doong, R., 2007. Dechlorination of carbon tetrachloride by ferrous ion associated with iron oxide nano particles. In: Proceedings of the Fourth Academic Sessions 2007.
Martín-González, L., Mortan, S.H., Rosell, M., Parladé, E., Martínez-Alonso, M., Gaju, N., Caminal, G., Adrian, L., Marco-Urrea, E., 2015. Stable carbon isotope fractionation during 1,2-dichloropropane-to-propene transformation by an enrichment culture containing *Dehalogenimonas* strains and a *dcpA* gene. Environ. Sci. Technol. 49, 8666–8674. https://doi.org/10.1021/acs.est.5b00929.
Matheson, L.J., Tratnyek, P.G., 1994. Reductive dehalogenation of chlorinated methanes by iron metal. Environ. Sci. Technol. 28, 2045–2053. https://doi.org/10.1021/es00061a012.
McGeough, K.L., Kalin, R.M., Myles, P., 2007. Carbon disulfide removal by zero valent iron. Environ. Sci. Technol. 41, 4607–4612. https://doi.org/10.1021/es062936z.
Morris, B.L., Lawrence, A.R.L., Chilton, P.J.C., Adams, B., Calow, C.R., Klinck, B.A., 2003. Groundwater and its Susceptibility to Degradation: a Global Assessment of the Problem and Options for Management. Early Warning and Assessment Report Series, RS. 03–3. United Nations Environment Programma, Nairobi, Kenya. https://doi.org/10.1d017/CBO9781107415324.004.
Nijenhuis, I., Renpenning, J., Kümmel, S., Richnow, H.H., Gehre, M., 2016. Recent advances in multi-element compound-specific stable isotope analysis of organohalides: achievements, challenges and prospects for assessing environmental sources and transformation. Trends Environ. Anal. Chem. 11, 1–8. https://doi.org/10.1016/j.teac.2016.04.001.
Obiri-Nyarko, F., Grajales-Mesa, S.J., Malina, G., 2014. An overview of permeable reactive barriers for in situ sustainable groundwater remediation. Chemosphere 111, 243–259. https://doi.org/10.1016/j.chemosphere.2014.03.112.
Palau, J., Marchesi, M., Chambon, J.C.C., Aravena, R., Canals, À., Binning, P.J., Bjerg, P.L., Otero, N., Soler, A., 2014. Multi-isotope (carbon and chlorine) analysis for fingerprinting and site characterization at a fractured bedrock aquifer contaminated by chlorinated ethenes. Sci. Total Environ. 475, 61–70. https://doi.org/10.1016/j.scitotenv.2013.12.059.
Pecher, K., Haderlein, S.B., Schwarzenbach, R.P., 2002. Reduction of polyhalogenated methanes by surface-bound Fe(II) in aqueous suspensions of iron oxides. Environ. Sci. Technol. 36, 1734–1741. https://doi.org/10.1021/es011191o.
Penny, C., Vuilleumier, S., Bringel, F., 2010. Microbial degradation of tetrachloromethane: mechanisms and perspectives for bioremediation. FEMS Microbiol. Ecol. 74, 257–275. https://doi.org/10.1111/j.1574-6941.2010.00935.x.
Peyton, T.O., Steel, R.V., Mabey, W.R., 1976. Carbon Disulfide, Carbonyl Sulfide: Literature Review and Environmental Assessment (EPA-600/9-78-009). Washington, DC.
Renpenning, J., Nijenhuis, I., 2016. Evaluation of the microbial reductive dehalogenation reaction using Compound-Specific Stable Isotope Analysis (CSIA). In: Adrian, L., Löffler, E.F. (Eds.), Organohalide-respiring Bacteria. Springer Berlin Heidelberg, Berlin, pp. 429–453. https://doi.org/10.1007/978-3-662-49875-0_18.
Rodríguez-Fernández, D., Torrentó, C., Guivernau, M., Viñas, M., Hunkeler, D., Soler, A., Domènech, C., Rosell, M., 2018. Vitamin B_{12} effects on chlorinated methanes-degrading microcosms: dual isotope and metabolically active microbial populations assessment. Sci. Total Environ. 621, 1615–1625. https://doi.org/10.1016/j.scitotenv.2017.10.067.
Scherer, M.M., Balko, B.A., Tratnyek, P.G., 1998. The role of oxides in reduction reactions at the metal-water interface. In: T, G. (Ed.), Kinetics and Mechanisms of Reactions at the Mineral/water Interface. ACS Symposium Series, Division of Geochemistry, Washington, DC, pp. 301–322.
Scheutz, C., Durant, N.D., Hansen, M.H., Bjerg, P.L., 2011. Natural and enhanced anaerobic degradation of 1,1,1-trichloroethane and its degradation products in the subsurface - a critical review. Water Res. 45, 2701–2723. https://doi.org/10.1016/j.watres.2011.02.027.
Song, H., Carraway, E.R., 2006. Reduction of chlorinated methanes by nano-sized zero-valent iron. Kinetics, pathways and effect of reaction conditions. Environ. Eng. Sci. 23, 272–284. https://doi.org/10.1089/ees.2006.23.272.
Svoronos, P.D.N., Bruno, T.J., 2002. Carbonyl Sulfide: a review of its chemistry and properties. Ind. Eng. Chem. Res. 41, 5321–5336. https://doi.org/10.1021/ie020365n.
Támara, M.L., Butler, E.C., 2004. Effects of iron purity and groundwater characteristics on rates and products in the degradation of carbon tetrachloride by iron metal. Environ. Sci. Technol. 38, 1866–1876. https://doi.org/10.1021/es0305508.
Thullner, M., Centler, F., Richnow, H.H., Fischer, A., 2012. Quantification of organic pollutant degradation in contaminated aquifers using compound specific stable isotope analysis - review of recent developments. Org. Geochem. 42, 1440–1460. https://doi.org/10.1016/j.orggeochem.2011.10.011.
Thullner, M., Fischer, A., Richnow, H.-H., Wick, L.Y., 2013. Influence of mass transfer on stable isotope fractionation. Appl. Microbiol. Biotechnol. 97, 441–452. https://doi.org/10.1007/s00253-012-4537-7.
Torrentó, C., Audí-Miró, C., Bordeleau, G., Marchesi, M., Rosell, M., Otero, N., Soler, A., 2014. The use of alkaline hydrolysis as a novel strategy for chloroform remediation: the feasibility of using construction wastes and evaluation of carbon isotopic fractionation. Environ. Sci. Technol. 48, 1869–1877. https://doi.org/10.1021/es403838t.
Torrentó, C., Palau, J., Rodríguez-Fernández, D., Heckel, B., Meyer, A., Domènech, C., Rosell, M., Soler, A., Elsner, M., Hunkeler, D., 2017. Carbon and chlorine isotope fractionation patterns associated with different engineered chloroform transformation reactions. Environ. Sci. Technol. 51, 6174–6184. https://doi.org/10.1021/acs.est.7b00679.
Van Breukelen, B.M., 2007. Extending the Rayleigh equation to allow competing isotope fractionating pathways to improve quantification of biodegradation. Environ. Sci. Technol. 41, 4004–4010. https://doi.org/10.1021/es0628452.
Vikesland, P.J., Heathcock, A.M., Rebodos, R.L., Makus, K.E., 2007. Particle size and aggregation effects on magnetite reactivity toward carbon tetrachloride. Environ. Sci. Technol. 41, 5277–5283. https://doi.org/10.1021/es062082i.
Vodyanitskii, Y.N., 2014. Effect of reduced iron on the degradation of chlorinated hydrocarbons in contaminated soil and ground water: a review of publications. Eurasian Soil Sci. 47, 119–133. https://doi.org/10.1134/S1064229314020136.
Zogorski, J.S., Carter, J.M., Ivahnenko, T., Lapham, W.W., Moran, M.J., Rowe, B.L., Squillace, P.J., Toccalino, P.L., 2006. The Quality of Our Nation's Waters - Volatile Organic Compounds in the Nation's Groundwater and Drinking-water Supply Wells. U.S. Geological Survey Circular 1292.
Zwank, L., Elsner, M., Aeberhard, A., Schwarzenbach, R.P., 2005. Carbon isotope fractionation in the reductive dehalogenation of carbon tetrachloride at iron (hydr)oxide and iron sulfide minerals. Environ. Sci. Technol. 39, 5634–5641. https://doi.org/10.1021/es0487776.